Inorg. Chem. **2007**, *46*, 10913–10925

Wurster's Crowns: A Comparative Study of *ortho*- and *para*-Phenylenediamine-Containing Macrocyclic Receptors

John W. Sibert,*,† Philip B. Forshee,† Greg R. Hundt,† Andrew L. Sargent,*,‡ Simon G. Bott,§ and Vincent Lynch||

Department of Chemistry, The University of Texas at Dallas, Richardson, Texas 75083, Department of Chemistry, East Carolina University, Greenville, North Carolina 27858, Department of Chemistry, University of Houston, Houston, Texas 77204, and Department of Chemistry, The University of Texas at Austin, Austin, Texas 78712

Received August 6, 2007

Two series of isomeric, redox-responsive azacrown ethers based on *ortho*- and *para*-phenylenediamine (Wurster's crowns) have been synthesized and their properties explored through ^{13}C NMR spectroscopy, electrospray ionization mass spectrometry, cyclic voltammetry, and X-ray crystallography. These crowns display strong affinity for alkali metal cations while maintaining comparable selectivity profiles to the parent crown ethers from which they are derived. Like Wurster's reagent (*N*,*N*,*N*′,*N*′-tetramethyl-*p*-phenylenediamine or *para*-TMPD), the *para*-Wurster's crowns undergo two reversible one-electron oxidations. The integrity of the alkali metal ion complexes is maintained in the neutral and singly oxidized ligand states but not after removal of two electrons. In contrast, the oxidation of *ortho*-Wurster's crowns is scan rate dependent, occurring at potentials substantially higher than their *para* counterparts, with their complexes oxidizing irreversibly. X-ray crystal structures of representative complexes show, in all cases, participation of the redox-active phenylenediamine subunits in complex formation via direct bonding to the guest cation.

Introduction

Since their discovery by Pederson in the late 1960s,[1] crown ethers have been the focus of numerous fundamental and applied studies. Their properties and coordination chemistry with alkali and alkaline earth metal cations are well documented and based on "hard−hard" type, electrostatic ion−dipole interactions with an established selectivity often attributed, albeit simplistically, to an optimal spatial fit between the macrocyclic cavity size and cationic radius.[2] Over the past three decades, there have been a variety of crown ethers reported that contain further functionality for the sensing of cationic guests. In particular, redox-active macrocycles in which an electrochemically active subunit is part of the host structure have received considerable attention.[3] In these systems, complexation triggers an electrochemical response from the macrocycle that is characteristic of the bound species. Alternatively, the coordination environment provided by the macrocycle can be altered by a change in oxidation state of the redox center giving rise to redox-switchable applications.[4] Early work focused primarily on crown ethers that contained the reducible nitrobenzyl[5] or quinone[6] groups. The complexation of cations resulted in more facile reduction of the redox center with the reduced form of the host forming stronger complexes with cationic guests. However, the enhanced binding came at the expense of cation selectivity. Other studies emphasized the incorporation of oxidizable redox centers with the vast majority of reported compounds containing either ferrocene[7] or tetrathi-

* To whom correspondence should be addressed. E-mail: sibertj@utdallas.edu.
† The University of Texas at Dallas.
‡ East Carolina University.
§ University of Houston.
|| The University of Texas at Austin.

(1) (a) Pedersen, C. J. *J. Am. Chem. Soc.* **1967**, *89*, 2495. (b) Pedersen, C. J. *J. Am. Chem. Soc.* **1967**, *89*, 7017. (c) Pedersen, C. J. *Angew. Chem.* **1988**, *100*, 1053.

(2) Bradshaw, J S.; Izatt, R. M.; Bordunov, A. V.; Zhu, C. Y.; Hathaway, J. K. In *Comprehensive Supramolecular Chemistry*; Gokel, G. W., Atwood, J. L., Davies, J. E., MacNicol, D. D., Vögtle, F., Eds.; Pergamon: Oxford, U.K., 1996; Vol. 1, pp 35−95.

(3) Kaifer, A. E.; Mendoza, S. In *Comprehensive Supramolecular Chemistry*; Gokel, G. W., Atwood, J. L., Davies, J. E., MacNicol, D. D., Vogtle, F., Eds.; Pergamon: Oxford, U.K., 1996; Vol. 1, pp 701−732.

(4) (a) Boulas, P. L.; Gomez-Kaifer, M.; Echegoyen, L. *Angew. Chem, Int. Ed. Engl.* **1998**, *37*, 216−247. (b) Saji, T.; Kinoshita, I. *J. Chem. Soc., Chem. Commun.* **1986**, 716−717.

10.1021/ic701560n CCC: $37.00
Published on Web 11/13/2007

afulvalene[8] (TTF). While ferrocene lacks ligating functionalities, its presence within a macrocyclic structure brings metal cations in close proximity to allow "through-space" interaction.[9] In addition, ferrocene-containing crowns have been developed which contain either ligating atoms attached directly to the cyclopentadienyl rings or a conjugated pathway between the ferrocene subunit and a macrocyclic donor atom for increased communication between the redox center and guest cations.[10] TTF-containing crown ethers also respond electrochemically to metal cations, though typically with modest changes in ligand oxidation potentials due, in part, to the relatively poor match of soft donor functionalities with hard cationic guests. Since a fundamental premise to both sensing and redox-switchable applications is a strong mutual interaction between the redox center and a bound guest, we became interested in macrocyclic receptors that facilitate the direct participation of the redox center in the stabilization of complexes.

Wurster's reagent, *p*-TMPD, and its *ortho* isomer (*o*-TMPD) are well-studied redox-active molecules that undergo two successive, reversible one-electron oxidations.[11] Both TMPD isomers contain amino groups, critical to the electrochemical activity of the molecules, which can potentially serve as donor atoms in the formation of metal complexes. As such, redox-active macrocycles based on phenylenediamine are well suited for facilitating the interaction between a bound metal ion and the redox center through a linking N atom integral to complex stability and redox activity.

We[12] and others[13−16] have described *para*-phenylenediamine-containing crown ethers which, inspired by their structural relationship to the well-known Wurster's reagent,[17] have been called "Wurster's crowns" (see Figure 1). Studies of these crowns revealed size selective encapsulation of metal cations and an ability to sense alkali metal cations both electrochemically[14c] and spectroscopically by fluorescence.[14b,16] In a more recent communication, we described the first *ortho*-Wurster's crown ether, an analog of 18-crown-6, and its K^+ complex.[18] Of note, the *ortho*-phenylenediamine subunit participates in the complex through bonding by both amino groups. It can thus be more correctly viewed as a redox-active lariat ether. The consequence of such a strong interaction was the observation of an unusually large shift in the oxidation potential of the crown upon treatment with K^+. While both *para* and *ortho*-Wurster's crown ethers share a similar structural motif, they contain redox centers with distinct ligating abilities and electrochemistry. A direct comparison of their properties both in solution and the solid state has yet to be reported. Therefore, we describe here the preparation of isomeric series of *ortho* and *para*-Wurster's crown ethers and report on their electrochemical properties and coordination chemistry.

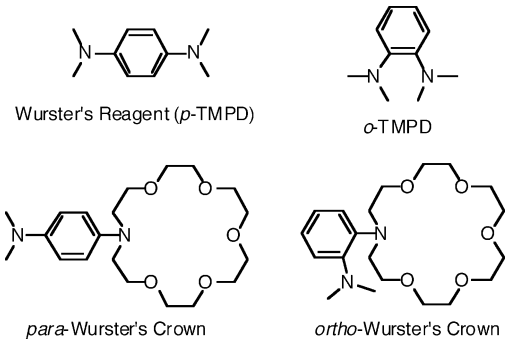

Figure 1. Wurster's reagent, *o*-TMPD, and representative *para*- and *ortho*-Wurster's crowns.

Experimental Section

Materials and Methods. Synthesis. All reactions were carried out under dry argon unless stated otherwise. Low-water solvents purchased form Burdick & Jackson were used in all preparations with the exception of ethyl acetate which was HPLC grade. All other commercially available reagents were used as purchased. Compounds **3**, **6**, and **9** were prepared using previously reported procedures.[18] Compounds **10**−**12** have been reported by Witulski using an alternate synthetic procedure.[19] As spectral characterization was not included in that work, we have reported it here. In addition, the precursor crowns **13** and **14** have been previously reported using alternate synthetic procedures.[20,21]

(5) (a) Gustowski, D. A.; Echegoyen, L.; Goli, D. M.; Kaifer, A.; Schultz, R. A.; Gokel, G. W. *J. Am. Chem. Soc.* **1984**, *106*, 1633−1635. (b) Kaifer, A.; Gustowski, D. A.; Echegoyen, L.; Gatto, V. J.; Schultz, R. A.; Cleary, T. P.; Morgan, C. R.; Goli, D. M.; Rios, A. M.; Gokel, G. W. *J. Am. Chem. Soc.* **1985**, *107*, 1958−1965. (c) Miller, S. R.; Gustowski, D. A.; Chen, Z. H.; Gokel, G. W.; Echegoyen, L.; Kaifer, A. E. *Anal. Chem.* **1988**, *60*, 2021−2024.
(6) (a) Gustowski, D. A.; Delgado, M.; Gatto, V. J.; Echegoyen, L.; Gokel, G. W. *J. Am. Chem. Soc.* **1986**, *108*, 7553−7560. (b) Delgado, M.; Gustowski, D. A.; Yoo, H. K.; Gatto, V. J.; Gokel, G. W.; Echegoyen, L. *J. Am. Chem. Soc.* **1988**, *110*, 119−124. (c) Chen, Z.; Schall, O. F.; Alcala, M.; Li, Y.; Gokel, G. W.; Echegoyen, L. *J. Am. Chem. Soc.* **1992**, *114*, 444−451.
(7) (a) Beer, P. D.; Gale, P. A.; Chen, Z. *Adv. Phys. Org. Chem.* **1998**, *31*, 1−90. (b) Beer, P. D. *Adv. Inorg. Chem.* **1992**, *39*, 79−157.
(8) (a) Le Derf, F.; Mazari, M.; Mercier, N.; Levillain, E.; Trippe, G.; Riou, A.; Richomme, P.; Becher, J.; Garin, J.; Orduna, J.; Gallego-Planas, N.; Gorgues, A.; Salle, M. *Chem.—Eur. J.* **2001**, *7*, 447−455. (b) Nielsen, M. B.; Lomholt, C.; Becher, J. *Chem. Soc. Rev.* **2000**, *29*, 153−164. (c) Jorgensen, T.; Hansen, T. K.; Becher, J. *Chem. Soc. Rev.* **1994**, *23*, 41−51.
(9) For an interesting exception involving direct interaction between the iron atom in ferrocene and a bound guest cation, see the following: Medina, J. C.; Goodnow, T. T.; Rojas, M. T.; Atwood, J. L.; Lynn, B. C.; Kaifer, A. E.; Gokel, G. W. *J. Am. Chem. Soc.* **1992**, *114*, 10583−10595.
(10) See, for examples the following: (a) Andrews, M. P.; Blackburn, C.; McAleer, J. F.; Patel, V. D. *J. Chem. Soc., Chem. Commun.* **1987**, 1122−1124. (b) Saji, T. *Chem. Lett.* **1986**, 275−276.
(11) Zweig, A.; Lancaster, J. E.; Neglia, M. T.; Jura, W. H. *J. Am. Chem. Soc.* **1964**, *86*, 4130−4136.
(12) (a) Sibert, J. W. U.S. Patent 6,262,258, 2001. (b) Sibert, J. W. U.S. Patent 6,441,164, 2002. (c) Sibert, J. W.; Forshee, P. B.; Lynch, V. *Inorg. Chem.* **2005**, *44*, 8602−8609. (d) Sibert, J. W.; Hundt, G. R.; Sargent, A. L.; Lynch, V. *Tetrahedron* **2005**, *61*, 12350−12357. (e) Sargent, A. L.; Mosley, B. J.; Sibert, J. W. *J. Phys. Chem. A.* **2006**, *110*, 3826−3837.
(13) Zhang, X.-X.; Buchwald, S. L. *J. Org. Chem.* **2000**, *65*, 8027−8031.
(14) (a) Pearson, A. J.; Hwang, J. *Tetrahedron Lett.* **2001**, *42*, 3533−3536. (b) Pearson, A. J.; Hwang, J.; Ignatov, M. E. *Tetrahedron Lett.* **2001**, *42*, 3537−3540. (c) Pearson, A. J.; Hwang, J. *Tetrahedron Lett.* **2001**, *42*, 3541−3543.
(15) Liu, X.; Eisenberg, A. H.; Stern, C. L.; Mirkin, C. A. *Inorg. Chem.* **2001**, *40*, 2940−2941.
(16) Crochet, P.; Malval, J.-P.; Lapouyade, R. *J. Chem. Soc., Chem. Commun.* **2000**, 289−290.
(17) Wurster, C. *Ber. Dtsch. Chem. Ges.* **1879**, *12*, 522−528.
(18) Sibert, J. W.; Forshee, P. B. *Inorg. Chem.* **2002**, *41*, 5928−5930.
(19) Witulski, B. *Synlett* **1999**, *8*, 1223−1226.
(20) Lu, X.-X.; Qin, S.-Y.; Zhou, Z.-Y.; Yam, V. W. *Inorg. Chim. Acta* **2003**, *346*, 49−56.
(21) Dix, J. P.; Vögtle, F. *Chem. Ber.* **1980**, *113*, 457−470.

NMR Spectroscopy. All ^{1}H and ^{13}C NMR spectra were recorded on a JEOL Eclipse 270 MHz NMR spectrometer in acetonitrile-d_3 or chloroform-*d* (Aldrich) using the solvent (δ = 7.26 ppm for $CHCl_3$, 77.0 ppm for $CDCl_3$, 1.96 ppm for CHD_2CN, 118.26 for CD_3CN) as an internal standard. Due to the low oxidation potential of the *para*-phenylenediamine-containing crown ethers **13**−**18**, NMR spectra occasionally showed broadened resonances due to the presence of a small amount of the crowns in their radical cationic form. In these cases, several grains of tetrabutylammonium borohydride or sodium borohydride were added to the NMR samples as in situ reducing agents. The former provided more consistent results as it has excellent solubility in deuterated chloroform and does not present a cation that would complex with the ligands studied. The latter has very limited solubility in deuterated chloroform and, thus, has the practical advantage of simply being filtered to regain the NMR sample in pure form. We note that in deuterated chloroform the formation of sodium complexes was never observed because of the poor solubility of sodium borohydride. Complexes of **7**−**9** and **16**−**18** with Li^+, Na^+, K^+, Rb^+, and Cs^+ were prepared by adding the ligand (ca. 20 mg), 1.25 equiv of either $LiBF_4$, $NaClO_4$, KPF_6, $RbClO_4$, or $CsClO_4$, and acetonitrile-d_3 (approximately 1 mL) to a vial that was then sonicated and heated to promote dissolution.

Caution: Perchlorate salts of metal complexes with organic ligands are potentially explosive.

Mass Spectrometry. Electrospray ionization (ESI-MS) mass spectra were measured using a Micromass Quatro II electrospray triple quadrapole mass spectrometer. Electron impact (EI) mass spectra were measured using a Fisions VG 70-250 SE mass spectrometer at Northwestern University. Competition experiments were performed by adding ligands **16**−**18** (approximately 20 mg each) to separate vials containing a stoichiometric excess (1.25 equiv) of $LiBF_4$, $NaClO_4$, KPF_6, $RbClO_4$, and $CsClO_4$ in 2 mL of CH_3CN. The resultant mixtures were subsequently sonicated and heated. Following the removal of solvent, the residues were triturated with CH_2Cl_2 and filtered prior to analysis by electospray mass spectrometry.

Electrochemistry. Acetonitrile (low-water 99.9+% grade, Burdick and Jackson) was distilled from CaH_2. Electrochemical grade tetraethylammonium tetrafluoroborate ($TEABF_4$) was purchased from Aldrich and used without further purification. Electrochemical experiments were conducted using a BAS CV-50W analyzer with a platinum disk working electrode, a platinum wire counter electrode, and a Ag/AgCl reference electrode. Potentials are cited versus the Ag/AgCl electrode. Acetonitrile solutions of ligands (approximately 4 mM) containing 0.1 M $(TEA)BF_4$ as a supporting electrolyte were placed in a single-compartment electrochemical cell and purged with nitrogen gas. A nitrogen atmosphere was maintained above the solution while the experiments were in progress. Coordination studies were performed by adding 2 equiv of $LiBF_4$, $NaClO_4$, KPF_6, $RbClO_4$, or $CsClO_4$ to approximately 4 mM acetonitrile solutions (0.1 M $(TEA)BF_4$) of either **7**, **8**, **9**, **16**, **17**, or **18**.

Computational Methods. Gas-phase molecular geometries were optimized with ab initio DFT methods that made use of Becke's three-parameter hybrid exchange functional (B3)[22] and the Lee−Yang−Parr correlation functional (LYP).[23] Following preliminary geometry optimizations with a standard 6-31G basis,[24] the molecular structures were refined with the 6-31+G* basis set.[25] Previous studies have demonstrated that electron-rich groups such as TMPD require a careful application of theory to accurately model the hybridization of the amine groups and their orientation with respect to the plane of the phenyl ring.[12e,26,27] In this context, the B3LYP/6-31+G* and UB3LYP/6-31+G* methods should be reliable for the neutral and radical cation forms of the Wurster's crowns, respectively. Analytical vibrational frequencies, scaled by 0.98 to obtain accurate zero-point energies,[28] were evaluated with the 6-31G basis and verified that all structures were local minima at this level of theory. Atomic charges were calculated by the natural population analysis (NPA)/natural bond orbital (NBO) method.[29] All calculations were performed with either the G94[30] or G98[31] program suite.

X-ray Crystallography. Crystals of **8**·$NaPF_6$ and **17**·$NaBF_4$ were sealed in glass capillaries under argon and mounted on the goniometer of a Bruker CCD SMART system, equipped with graphite-monochromated Mo Kα radiation (λ = 0.710 73 Å), and corrected for Lorentz and polarization effects. Data collection and unit cell and space group determination were all carried out using methods reported previously.[32] The structure was solved by direct methods (SHELXTL),[33] and the model was refined using full-matrix least-squares techniques.[34] All hydrogen atoms were placed in calculated positions [U_{iso} = 1.3U(C); d(C−H) = 0.95 Å] for refinement. Refinement of positional and anisotropic thermal parameters led to convergence.

The data for crystals of **8**·KPF_6 and **9**·$LiBF_4$ were collected on a Nonius Kappa CCD diffractometer using a graphite monochromator with Mo Kα radiation (λ = 0.710 73 Å) at 153 K using an Oxford Cryostream low-temperature device. Data reduction were performed using DENZO-SMN.[35] The structure was solved by

(22) Becke, A. D. *J. Chem. Phys.* **1993**, *98*, 5648−5652.
(23) Lee, C.; Yang, W.; Parr, R. G. *Phys. Rev. B* **1988**, *37*, 785−789.
(24) Ditchfield, R.; Hehre, W. J.; Pople, J. A. *J. Chem. Phys.* **1971**, *54*, 724−728. (b) Hehre, W. J.; Ditchfield, R.; Pople, J. A. *J. Chem. Phys.* **1972**, *56*, 2257−2261.
(25) (a) Clark, T.; Chandrasekhar, J.; Spitznagel, G. W.; Schleyer, P. v. R. *J. Comput. Chem.* **1983**, *4*, 294−301. (b) Frisch, M. J.; Pople, J. A.; Binkley, J. S. *J. Chem. Phys.* **1984**, *80*, 3265−3269.
(26) (a) Brouwer, A. M.; Wilbrandt, R. *J. Phys. Chem.* **1996**, *100*, 9678−9688. (b) Brouwer, A. M. *J. Phys. Chem. A* **1997**, *101*, 3626−3633.
(27) Sponer, J.; Hobza, P. *Int. J. Quantum Chem.* **1996**, *57*, 959−970.
(28) (a) Bauchlicher, C. W.; Partridge, H. *J. Chem. Phys.* **1995**, *103*, 1788−1791. (b) Wong, M. W. *Chem. Phys. Lett.* **1996**, *256*, 391−399.
(29) Reed, A. E.; Curtiss, L. A.; Weinhold, F. *Chem. Rev.* **1988**, *88*, 899−926.
(30) Frisch, M. J.; Trucks, G. W.; Schlegel, H. B.; Gill, P. M. W.; Johnson, B. G.; Robb, M. A.; Cheeseman, J. R.; Keith, T. A.; Petersson, G. A.; Montgomery, J. A.; Raghavachari, K.; Al-Laham, M. A.; Zakrzewski, V. G.; Ortiz, J. V.; Foresman, J. B.; Cioslowski, J.; Stefanov, B. B.; Nanayakkara, A.; Challacombe, M.; Peng, C. Y.; Ayala, P. Y.; Chen, W.; Wong, M. W.; Andres, J. L.; Replogle, E. S.; Gomperts, R.; Martin, R. L.; Fox, D. J.; Binkley, J. S.; Defrees, D. J.; Baker, J.; Stewart, J. J. P.; Head-Gordon, M.; Gonzalez, C.; Pople, J. A. *Gaussian 94*, revision D1; Gaussian, Inc.: Pittsburgh, PA, 1995.
(31) Frisch, M. J.; Trucks, G. W.; Schlegel, H. B.; Scuseria, G. E.; Robb, M. A.; Cheeseman, J. R.; Zakrzewski, V. G.; Montgomery, J. A., Jr.; Stratmann, R. E.; Burant, J. C.; Dapprich, S.; Millam, J. M.; Daniels, A. D.; Kudin, K. N.; Strain, M. C.; Farkas, O.; Tomasi, J.; Barone, V.; Cossi, M.; Cammi, R.; Mennucci, B.; Pomelli, C.; Adamo, C.; Clifford, S.; Ochterski, J.; Petersson, G. A.; Ayala, P. Y.; Cui, Q.; Morokuma, K.; Malick, D. K.; Rabuck, A. D.; Raghavachari, K.; Foresman, J. B.; Chioslowski, J.; Ortiz, J. V.; Baboul, A. G.; Stefanov, B. B.; Liu, G.; Liashenko, A.; Piskorz, P.; Komaromi, I.; Gomperts, R.; Martin, R. L.; Fox, D. J.; Keith, T.; Al-Laham, M. A.; Peng, C. Y.; Nanayakkara, A.; Challacombe, M.; Gill, P. M. W.; Johnson, B.; Chen, W.; Wong, M. W.; Andres, J. L.; Gonzalez, C.; Head-Gordon, M.; Replogle, E. S.; Pople, J. A. *Gaussian 98*, revision A.9; Gaussian Inc.: Pittsburgh, PA, 1998.
(32) Mason, M. R.; Smith, J. M.; Bott, S. G.; Barron, A. R. *J. Am. Chem. Soc.* **1993**, *115*, 4971.
(33) Sheldrick, G. M. *Acta Crystallogr., Sect. A* **1990**, *46*, 467.
(34) Sheldrick, G. M. *SHELXTL*; Bruker Corp.: Madison, WI.

Table 1. Summary of Crystallographic Data

param	**17**·$NaBF_4$	**8**·$NaPF_6$	**8**·KPF_6	**9**·$LiBF_4$
empirical formula	$C_{18}H_{30}BF_4N_2NaO_4$	$C_{18}H_{30}F_6N_2NaO_4P$	$C_{18}H_{30}F_6KN_2O_4P$	$C_{20}H_{38}BF_4LiN_2O_7$
mol wt	484.24	506.40	522.51	521.27
cryst system	monoclinic	monoclinic	triclinic	monoclinic
space group	$P2_1/n$	$P2_1/c$	$P\bar{1}$ (No. 2)	$P2_1/n$
a (Å)	8.161(2)	10.5135(2)	9.815(2)	11.3765(3)
b (Å)	12.543(3)	20.3407(3)	11.750(2)	12.1450(3)
c (Å)	21.773(4)	11.1139(4)	12.481(3)	18.5284(4)
α (deg)	90.00	90.00	62.83(3)	90.00
β (deg)	96.29(3)	103.114(1)	80.69(3)	95.049(1)
γ (deg)	90.00	90.00	65.93(3)	90.00
V (Å^3)	2215.3(8)	2314.75(7)	1168.7(4)	2550.09(11)
Z	4	4	2	4
temp (K)	293(2)	293(2)	293(2)	153(2)
ρ_{calcd} (g·cm^{-3})	1.344	1.453	1.485	1.334
μ (mm^{-1})	0.131	0.213	0.370	0.115
GOF on F^2	1.001	1.142	1.023	1.051
final R indices [$I > 2\sigma(I)$]				
R1	0.0520	0.0469	0.0579	0.0582
wR2	0.1338	0.1086	0.1631	0.1259
R indices (all data)				
R1	0.0977	0.0844	0.0639	0.1091
wR2	0.1517	0.1237	0.1711	0.1443

direct methods using SIR97[36] and refined by full-matrix least squares on F^2 with anisotropic displacement parameters for the non-H atoms using SHELXL-97.[37] The hydrogen atoms on carbon were calculated in ideal positions with isotropic displacement parameters set to $1.2U_{eq}$ of the attached atom ($1.5U_{eq}$ for methyl hydrogen atoms).

In the case of **8**·KPF_6, crystals grew as large, colorless prisms by slow evaporation from pentane−chloroform solution. The data crystal was cut from a much larger crystal and had approximate dimensions 0.42 × 0.29 × 0.23 mm. A total of 448 frames of data were collected using ω-scans with a scan range of 1° and a counting time of 38 s/frame. The hexafluorophosphate anion was disordered about two principal orientations. The disorder was modeled by first restraining the geometry of the two groups to be approximately equal. The site occupancy of the two orientations were refined so that one orientation had a site occupancy set to the variable x and the other had a site occupancy set to $1 - x$. A common isotropic displacement parameter was refined for all fluorine and phosphorus atoms. The site occupancy for the major component of the disorder refined to 0.75(2). The minor component was composed of atoms P1a, F1a, F2a, F3a, F4a, F5a, and F6a. The geometric restraints were retained throughout the refinement procedure. Anistropic displacement parameters for the atoms of the anion were restrained to be approximately isotropic in the final refinement stages.

For **9**·$LiBF_4$, the data crystal was a long lath that had approximate dimensions 0.45 × 0.30 × 0.20 mm. A total of 455 frames of data were collected using ω-scans with a scan range of 1° and a counting time of 137 s/frame. A portion of the crown ether was found to be disordered about two orientations. The disorder involved two CH_2-CH_2O groups that were adjacent to the nitrogen atom in the crown. The disorder was modeled so that the sum of the site occupancy for an atom in one orientation plus the site occupancy factor for the related atom in the second orientation was equal to unity. Also, it was assumed that all the atoms in one orientation had the same site occupancy factor. The site occupancy factor of the major component of the disorder comprised atoms O13, C14, C15, O16, C17, and C18 refined to 55(2)% while simultaneously refining a common isotropic displacement parameter. The lower occupancy group was comprised of atoms O13a, C14a, C15a, O16a, C17a, and C18a. The geometry of the two groups was restrained to be equivalent throughout the refinement. While the non-H atoms of the disordered moieties were refined anisotropically, their displacement parameters were restrained to be isotropic.

Details of crystal data, data collection, and structure refinement are listed in Table 1.

Synthesis and Characterization. General Procedure for the Preparation of 2-Nitrophenyl-1-azacrown Ethers 1 and 2. Compounds **1** and **2** were prepared from the reaction of aza-12-crown-4 and aza-15-crown-5, respectively, with excess 2-fluoro-1-nitrobenzene using the procedure previously reported for **3**.[18] Compound **1**: yield 100% (based on crown); ^{1}H NMR ($CDCl_3$) δ 3.43 (4H, t, CH_2N, J = 5.0 Hz), 3.66 (12H, m, CH_2O), 6.88 (1H, t, Ar-*H*, J = 7.3 Hz), 7.40 (2H, m, Ar-*H*), 7.59 (1H, d, Ar-*H*, J = 8.3 Hz); ^{13}C NMR ($CDCl_3$) δ 52.72, 68.60, 69.52, 70.23, 118.91, 122.76, 124.55, 132.10, 141.48, 143.33; MS(ESI) m/z 297 (M + H^+). Compound **2**: yield 100% (based on crown); ^{1}H NMR ($CDCl_3$) δ 3.42 (4H, t, CH_2N, J = 5.9 Hz), 3.64 (16H, m, CH_2O), 6.90 (1H, t, Ar-*H*, J = 7.7 Hz), 7.35 (2H, m, Ar-*H*), 7.61 (1H, d, Ar-*H*, J = 8.3 Hz); ^{13}C NMR ($CDCl_3$) δ 53.67, 69.65, 70.52, 71.04, 120.34, 122.95, 125.69, 132.85, 142.98, 144.76; MS(ESI) m/z 341 (M + H^+).

General Procedure for the Preparation of 2-Aminophenyl-1-azacrown Ethers 4 and 5. Compounds **4** and **5** were prepared by the catalytic reduction of **1** and **2**, respectively, using the procedure previously reported for **6**.[18] Compound **4**: yield 96%; ^{1}H NMR ($CDCl_3$) δ 3.11 (4H, t, CH_2N, J = 4.5 Hz), 3.54 (4H, t, CH_2O, J = 4.5 Hz), 3.69 (8H, m, CH_2O), 6.66 (2H, m, Ar-*H*), 6.90 (1H, t, Ar-*H*, J = 7.9 Hz), 7.03 (1H, d, Ar-*H*, J = 7.7 Hz); ^{13}C NMR ($CDCl_3$) δ 54.14, 68.93, 70.78, 71.42, 115.32, 117.17, 122.67, 125.09, 136.89, 144.81. MS(ESI) m/z 267 (M + H^+). Compound **5**: yield 99%; ^{1}H NMR ($CDCl_3$) δ 3.15 (4H, t, CH_2N, J = 5.0 Hz), 3.48 (4H, t, CH_2O, J = 5.3 Hz), 3.65 (12H, m, CH_2O),

(35) For DENZO-SMN, see the following: Otwinowski, Z.; Minor, W. In *Methods in Enzymolology, Vol. 276: Macromolecular Crystallography*; Carter, C. W., Jr., Sweet, R. M., Eds.; Academic Press: New York, 1997; Part A, pp 307−326.

(36) For SIR97, a program for crystal structure solution, see the following: Altomare, A.; Burla, M. C.; Camalli, M.; Cascarano, G. L.; Giacovazzo, C.; Guagliardi, A.; Moliterni, A. G. G.; Polidori, G.; Spagna, R. *J. Appl. Crystallogr.* **1999**, *32*, 115−119.

(37) Sheldrick, G. M. *SHELXL97. Program for the Refinement of Crystal Structures*; University of Gottingen: Gottingen, Germany, 1994.

6.66 (2H, m, Ar-*H*), 6.90 (1H, t, Ar-*H*, $J = 7.7$ Hz), 7.05 (1H, d, Ar-*H*, $J = 7.9$ Hz); ^{13}C NMR ($CDCl_3$) δ 55.19, 69.35, 70.22, 70.63, 70.78, 115.13, 117.61, 123.66, 125.48, 137.06, 145.40; MS(ESI) *m*/*z* 311 ($M + H^+$).

General Procedure for the Preparation of 2-(Dimethylamino)-phenyl-1-azacrown Ethers 7 and 8. Compounds **7** and **8** were prepared by the methylation of **4** and **5**, respectively, using the procedure previously reported for **9**.[18] Compound **7**: yield 91%; ^{1}H NMR ($CDCl_3$) δ 2.74 (6H, s, C*H*$_3$N), 3.49 (4H, t, C*H*$_2$N, $J = 4.8$ Hz), 3.71 (12H, m, C*H*$_2$O), 6.91 (3H, m, Ar-*H*), 7.07 (1H, m, Ar-*H*); ^{13}C NMR ($CDCl_3$) δ 42.08, 51.40, 70.11, 70.52, 71.03, 118.18, 121.03, 121.73, 143.81, 146.24; MS(EI) *m*/*z* 294.2 (M^+); HRMS(EI) *m*/*z* 294.191 63 (M^+) (calcd for $C_{16}H_{26}N_2O_3$, *m*/*z* 294.194 34). Compound **8**: yield 90%; ^{1}H NMR ($CDCl_3$) δ 2.70 (6H, s, C*H*$_3$N), 3.45 (4H, t, C*H*$_2$N, $J = 4.8$ Hz), 3.64 (16H, m, C*H*$_2$O), 6.92 (3H, m, Ar-*H*), 7.09 (1H, m, Ar-*H*); ^{13}C NMR ($CDCl_3$) δ 42.03, 51.12, 70.11, 70.37, 70.66, 71.03, 118.32, 121.05, 121.65, 122.04, 143.15, 146.30; MS(EI) *m*/*z* 338.2 (M^+); HRMS(EI) *m*/*z* 338.221 71 (M^+) (calcd for $C_{18}H_{30}N_2O_4$, *m*/*z* 338.220 56).

General Procedure for the Preparation of 4-Nitrophenyl-1-azacrown Ethers 10−12. A mixture of 4-fluoro-1-nitrobenzene (5.0 equiv), the appropriate azacrown ether (1.0 equiv of aza-12-crown-4 for **10**, aza-15-crown-5 for **11**, and aza-18-crown-6 for **12**), and cesium carbonate (1.0 equiv) in DMF (10 mL/g of crown) was heated to 100 °C and stirred for 16 h under an argon atmosphere. The DMF was distilled in vacuo to leave a viscous oil which was partitioned between dichloromethane and water. The organic layer was separated, dried over $MgSO_4$, and concentrated to provide an orange oil that was further purified via column chromatography (silica gel eluted with 5% MeOH−$CHCl_3$). Compound **10**: yield 92%; ^{1}H NMR ($CDCl_3$) δ 3.58 (8H, m, C*H*$_2$O), 3.64 (4H, t, C*H*$_2$O, $J = 4.7$ Hz), 3.87 (4H, t, C*H*$_2$N, $J = 4.7$ Hz), 6.68 (2H, d, Ar-*H*, $J = 9.4$ Hz), 8.03 (2H, d, Ar-*H*, $J = 9.4$ Hz); ^{13}C NMR ($CDCl_3$) δ 52.91, 69.17, 69.87, 71.45, 111.20, 126.08, 137.11, 153.57; MS(ESI) *m*/*z* 297 ($M + H^+$). Compound **11**: yield 86%; ^{1}H NMR ($CDCl_3$) δ 3.55−3.70 (16H, m, C*H*$_2$O), 3.76 (4H, t, C*H*$_2$N, $J = 5.4$ Hz), 6.59 (2H, d, Ar-*H*, $J = 9.4$ Hz), 8.05 (2H, d, Ar-*H*, $J = 9.2$ Hz); ^{13}C NMR ($CDCl_3$) δ 53.13, 68.00, 69.94, 70.32, 71.26, 110.38, 126.21, 136.96, 152.49; MS(EI) *m*/*z* 339.1 ($M - 1^+$). Compound **12**: yield 87%; ^{1}H NMR ($CDCl_3$) δ 3.57−3.75 (24H, m, C*H*$_2$O, C*H*$_2$N), 6.68 (2H, d, Ar-*H*, $J = 8.9$ Hz), 8.08 (2H, d, Ar-*H*, $J = 9.1$ Hz); ^{13}C NMR ($CDCl_3$) δ 51.72, 68.18, 70.69, 70.77, 110.66, 126.18, 137.10, 152.60; MS(ESI) *m*/*z* 385 ($M + H^+$).

General Procedure for the Preparation of 4-Aminophenyl-1-azacrown Ethers 13−15. A mixture containing the appropriate 4-nitrophenyl-1-azacrown ether (**10** for **13**, **11** for **14**, and **12** for **15**) and 10% Pd/C (10 mol %) in ethyl acetate (20 mL/g of crown) was stirred under a H_2 atmosphere for 24 h. The solid catalyst was removed via filtration and rinsed with ethyl acetate. The filtrate was evaporated under reduced pressure to yield the desired crown. Compound **13**: yield 98%; ^{1}H NMR ($CDCl_3$) δ 3.49 (4H, t, C*H*$_2$N, $J = 6.4$ Hz), 3.61−3.68 (8H, m, C*H*$_2$O), 3.71 (4H, t, C*H*$_2$O, $J = 6.4$ Hz), 6.59 (4H, m, Ar-*H*); ^{13}C NMR ($CDCl_3$) δ 53.40, 70.03, 70.19, 71.63, 114.86, 116.86, 137.05, 142.65; MS(ESI) *m*/*z* 267 ($M + H^+$). Compound **14**: yield 97%; ^{1}H NMR ($CDCl_3$) δ 3.44 (4H, t, C*H*$_2$N, $J = 5.0$ Hz), 3.60−3.67 (12H, m, C*H*$_2$O), 3.79 (4H, t, C*H*$_2$O, $J = 5.0$ Hz), 6.59 (4H, m, Ar-*H*); ^{13}C NMR ($CDCl_3$) δ 52.68, 68.97, 70.22, 71.22, 113.34, 117.02, 136.40, 141.53; MS-(ESI) *m*/*z* 311 ($M + H^+$). Compound **15**: yield 100%; ^{1}H NMR ($CDCl_3$) δ 3.49 (4H, t, C*H*$_2$N, $J = 5.9$ Hz), 3.61−3.72 (20H, m, C*H*$_2$O), 6.62 (4H, m, Ar-*H*); ^{13}C NMR ($CDCl_3$) δ 52.16, 69.03, 70.54, 70.77, 114.57, 117.06, 136.62, 141.87; MS(EI) *m*/*z* 354.2 (M^+).

General Procedure for the Preparation of 4-(Dimethylamino)-phenyl-1-azacrown Ethers 16−18. A slurry of the appropriate 4-aminophenyl-1-azacrown ether (1.0 equiv of **13** for **16**, **14** for **17**, and **15** for **18**) and finely crushed sodium borohydride (8.0 equiv) in tetrahydrofuran (25 mL/g of crown) was added dropwise to a stirred mixture of 3 M sulfuric acid (1.5 mL) and 37% aqueous formaldehyde (5.0 equiv) in tetrahydrofuran at 10 °C. After half of the crown mixture was added, the reaction was further acidified with 3 M H_2SO_4 (1.5 mL) and the addition then continued until complete. Following the addition of water, solid KOH was added until the mixture was strongly basic. The reaction mixture was then placed in a separatory funnel and the organic layer removed. Two subsequent ether extractions of the aqueous layer were combined with the THF solution, and following drying with sodium sulfate, the solvents were removed in vacuo. The crude reaction product was then purified by column chromatography (neutral alumina eluted with 2% MeOH−$CHCl_3$). Compound **16**: yield 79%; ^{1}H NMR ($CDCl_3$) δ 2.76 (6H, s, C*H*$_3$N), 3.40 (4H, t, C*H*$_2$N, $J = 4.9$ Hz), 3.56 (8H, m, C*H*$_2$O), 3.71 (4H, t, C*H*$_2$O, $J = 4.7$ Hz), 6.70 (4H, m, Ar-*H*); ^{13}C NMR ($CDCl_3$) δ 42.21, 53.18, 69.94, 70.03, 71.58, 114.38, 115.69, 141.78, 143.22; MS(EI) *m*/*z* 294.2 (M^+); HRMS(EI) *m*/*z* 294.194 27 (M^+) (calcd for $C_{16}H_{26}N_2O_3$, *m*/*z* 294.194 34). Compound **17**: yield 72%; spectroscopic data consistent with those reported previously.[13] Compound **18**: yield 89%; ^{1}H NMR ($CDCl_3$) δ 2.81 (6H, s, C*H*$_3$N), 3.52 (4H, t, C*H*$_2$N, $J = 4.9$ Hz), 3.60−3.78 (20H, m, C*H*$_2$O), 6.73 (4H, m, Ar-*H*); ^{13}C NMR ($CDCl_3$) δ 42.21, 51.95, 69.11, 70.55, 70.73, 114.14, 115.84, 141.78, 143.22; ^{13}C NMR (CD_3CN) δ 42.17, 52.80, 69.80, 71.25, 71.31, 115.46, 116.33, 142.75, 144.30; MS(EI) *m*/*z* 382.2 (M^+); HRMS-(EI) *m*/*z* 382.247 08 (M^+) (calcd for $C_{20}H_{34}N_2O_5$, *m*/*z* 382.246 79).

Results and Discussion

Ligand Syntheses. As shown in Scheme 1, the new *ortho*-Wurster's crown ethers **7** and **8** were prepared by the method originally reported for **9**. This three-step synthesis begins with near quantitative nucleophilic aromatic substitution reactions involving azacrown ethers and 2-fluoro-1-nitrobenzene and produces the final target macrocycles in overall yields approaching 90%.

Within the past 5 years, there have been several methods developed to prepare *N*,*N*′-peralkylated-*para*-phenylenediamine-containing crown ether structures. Our previously reported procedure involved the condensation of the commercially available *N*,*N*-dimethyl-*p*-phenylenediamine with pentaethylene glycol ditosylate to give the Wurster's crown **18** in modest yield (typically 20%).[12a] While the yield is relatively low, this approach is not without merit as the reactants are inexpensive or easily prepared and do not include a preformed azacrown ether. Buchwald and co-workers have coupled aza-15-crown-5 with various aryl bromide derivatives using Pd-catalyzed amination chemistry to produce a range of aniline-containing crown ethers, including **17** in 84% yield.[13] A similar approach was used to generate the *meta*-Wurster's crown ethers in excellent yields.[38] Alternatively, Pearson and co-workers prepared

(38) Sibert, J. W.; Seyer, D. J.; Hundt, G. R. *J. Supramol. Chem.* **2002**, *2*, 335−342.

Scheme 1. Synthetic Outline for Ligands in This Study[a]

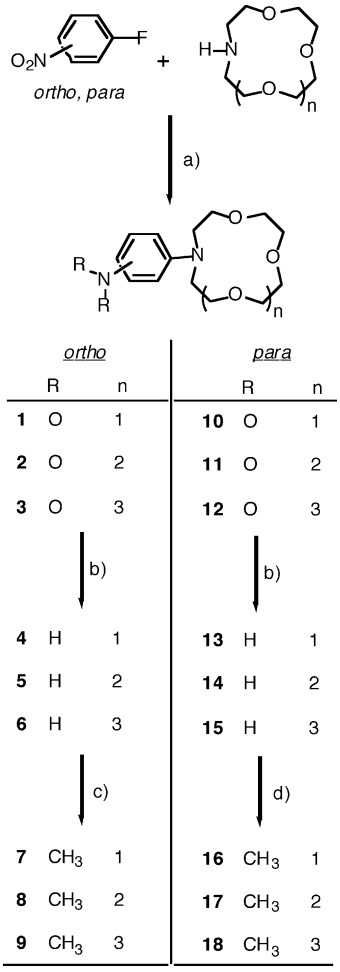

ortho			para		
	R	n		R	n
1	O	1	**10**	O	1
2	O	2	**11**	O	2
3	O	3	**12**	O	3
4	H	1	**13**	H	1
5	H	2	**14**	H	2
6	H	3	**15**	H	3
7	CH_3	1	**16**	CH_3	1
8	CH_3	2	**17**	CH_3	2
9	CH_3	3	**18**	CH_3	3

[a] Reagents: (a) Cs_2CO_3; (b) H_2, 10% Pd/C; (c) CH_3I, Cs_2CO_3; (d) CH_2O, $NaBH_4$, H_2SO_4.

piperidine derivatives of *p*-phenylenediamine-containing crown ethers from azacrown ethers by sequential S_NAr reactions on (*p*-dichlorobenzene)RuCp cationic complexes with overall yields of 26 and 37% for analogs of **17** and **18**, respectively.[14a] Finally, Lapouyade and co-workers have described a four step synthetic approach to crowned dimers of aniline, which contain either *m*- or *p*-phenylenediamine subunits.[16,39]

In this work, we have synthesized *para*-Wurster's crowns **16**−**18** in a manner analogous to that used for the *ortho* isomers and for a related Wurster's thiacrown ether that we recently reported.[40] We have found this procedure to be efficient and scalable. As shown in Scheme 1, reaction of either aza-12-crown-4, aza-15-crown-5, or aza-18-crown-6 with 4-fluoro-1-nitrobenzene produced **10**−**12**, respectively. Alternate routes to **10**−**12** have been reported by Witulski[19] and to **11** by Urgaonkar and Verkade[41] via palladium-catalyzed coupling of azacrown ethers to 4-bromo-1-nitrobenzene or 4-chloro-1-nitrobenzene. Reduction of the nitro functionality was achieved by catalytic hydrogenation to form **13**−**15**. The methylation procedure of Giumanini et al.[42] gave the desired final compounds **16**−**18** in unoptimized overall yields of 71, 60, and 77%, respectively, following chromatography on alumina.

NMR Spectroscopy. The coordination chemistry of *ortho*-Wurster's crowns with alkali metal cations was studied by ^{13}C NMR spectroscopy. As summarized in Table 2, spectra of **7**−**9** as free ligands and in the presence of $LiBF_4$, $NaClO_4$, KPF_6, $RbClO_4$, and $CsClO_4$ were acquired in deuterated acetonitrile. Several general trends are notable. Upon complexation, the methylene resonances next to the O atoms in all cases shift upfield. Such a shift is characteristic of metal complexes of crown ethers and is attributed to conformational changes in the crown upon complexation.[43] The methylene resonances next to the macrocyclic N atom and the methyl resonances are shifted downfield indicating strong participation of the redox center as a ligating entity through both amino groups. In addition, the aromatic carbon resonances are, on average, shifted downfield as the bound metal cation draws electron density from the phenyl ring via the two phenylenediamine N atoms. The magnitudes of these shifts are an indicator of the degree in which the crowns interact with guest cations. As expected then, the differing crown sizes in **7**−**9** give rise to unique spectral responses for the five alkali metal cations. For example, large shifts in the resonances of the smallest crown **7** occur upon complexation with Li^+ and Na^+ with minimal to no change observed for K^+, Rb^+, and Cs^+. A comparison of the ^{13}C NMR spectra for the alkali metal complexes of **8** shows, again, large shifts in the ^{13}C resonances for both Li^+ and Na^+ with more modest but significant shifts for K^+. While the Li^+ and Na^+ complexes of **8** give spectra that are similar to their complexes with **7**, the ^{13}C resonances next to the macrocyclic and dimethylamino N atoms are more substantially shifted in **8**. For the largest crown studied, **9**, an analog of the K^+-selective 18-crown-6, the spectrum of the K^+ complex contains ^{13}C resonances that are the most shifted. Interestingly, while Na^+ and Rb^+ complexes with **9** are clearly supported by the ^{13}C NMR data, the small Li^+ cation also interacts strongly with this larger macrocycle. In summary, the macrocyclic cavity sizes in these crowns play an important role in complex formation. Further, *ortho*-Wurster's crowns appear to have a general pronounced affinity for Li^+ via preferential interaction with the *ortho*-phenylenediamine moiety.

The ^{13}C NMR spectra of the *para*-Wurster's crowns are as expected for hybrid structures of *para*-phenylenediamine and crown ethers. The formal replacement of one dimethylamino group of *p*-TMPD with a crown moiety lowers the symmetry of the phenylenediamine moiety producing four discrete aromatic resonances. The ^{13}C NMR data for **16**−**18** and their alkali metal complexes are shown in Table 3. As in the metal complexes of *ortho*-Wurster's crowns, the ^{13}C resonances for the methylenes next to the O atoms are generally shifted upfield in the complexes of the *para*

(39) Malval, J. P.; Chaimbault, C.; Fischer, B.; Morand, J. P.; Lapouyade, R. *Res. Chem. Intermed.* **2001**, *27*, 21−34.
(40) Sibert, J. W.; Forshee, P. B.; Lynch, V. *Inorg. Chem.* **2005**, *44*, 8602−8609.
(41) Urgaonkar, S.; Verkade, J. G. *Tetrahedron* **2004**, *60*, 11837−11842.
(42) Giumanini, A. G.; Chiavari, G.; Musiani, M. M.; Rossi, P. *Synthesis* **1980**, *9*, 743−746.
(43) Dale, J. *Isr. J. Chem.* **1980**, *20*, 3−11.

Table 2. ^{13}C NMR Chemical Shift Data (ppm) for **7**−**9** and Associated Metal Complexes[a]

compd	C_1,C_2(av)[b]	C_3−C_6(av)[b]	$\mathbf{CH_2}$O(av)	$\mathbf{CH_2}$N	$\mathbf{CH_3}$N
7	146.45	121.78	71.27	52.65	42.65
+ $LiBF_4$	149.67	127.80	68.22	55.25	47.16
+ $NaClO_4$	149.66	126.76	67.08	54.45	47.00
+ KPF_6	146.79	122.28	70.76	52.76	43.01
+ $RbClO_4$	146.46	121.78	71.27	52.65	42.65
+ $CsClO_4$	146.47	121.78	71.29	52.65	42.65
8	145.82	121.69	70.98	52.22	42.38
+ $LiBF_4$	149.72	127.20	68.66	55.52	48.42
+ $NaClO_4$	150.07	127.06	68.86	56.51	47.22
+ KPF_6	149.55	125.50	69.38	55.78	45.58
+ $RbClO_4$	146.06	121.93	70.92	52.46	42.57
+ $CsClO_4$	145.95	121.81	70.98	52.35	42.48
9	145.72	121.69	70.92	51.84	42.32
+ $LiBF_4$	149.31	127.02	70.20	56.56	47.51
+ $NaClO_4$	149.10	125.24	70.09	55.63	46.31
+ KPF_6	150.59	126.35	70.43	58.71	47.16
+ $RbClO_4$	149.57	125.14	70.46	57.15	45.73
+ $CsClO_4$	147.93	123.88	70.47	51.92	42.37

[a] Measured in CD_3CN. [b] C_1−C_6 are designated as 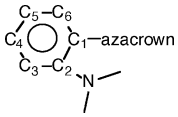

Table 3. ^{13}C NMR Chemical Shift Data (ppm) for **16**−**18** and Associated Metal Complexes[a]

compd	C_1[b]	C_4[b]	C_2−C_3(av)[b]	$\mathbf{CH_2}$O(av)	$\mathbf{CH_2}$N	$\mathbf{CH_3}$N
16	144.28	142.75	115.72	71.01	53.42	42.20
+ $LiBF_4$	150.26	140.19	119.49	67.50	54.29	40.88
+ $NaClO_4$	147.30	141.97	117.93	67.62	53.29	41.33
+ KPF_6	145.62	142.44	116.75	69.05	53.06	41.81
+ $RbClO_4$	144.40	142.75	115.81	70.88	53.42	42.19
+ $CsClO_4$	144.40	142.74	115.80	70.84	53.40	42.17
17	144.11	141.89	115.38	70.63	53.44	42.27
+ $LiBF_4$	149.58	137.98	120.12	68.86	56.22	40.90
+ $NaClO_4$	149.72	138.36	120.31	69.27	57.02	40.92
+ KPF_6	147.24	141.63	118.04	69.19	55.58	41.38
+ $RbClO_4$	145.16	142.02	116.29	70.05	54.28	41.95
+ $CsClO_4$	144.68	142.10	115.88	70.17	53.99	42.06
18	144.52	142.06	115.86	70.80	52.76	42.17
+ $LiBF_4$	148.45	139.22	119.06	69.62	55.12	41.22
+ $NaClO_4$	148.77	141.00	119.43	69.46	55.23	41.16
+ KPF_6	150.07	137.99	120.73	70.28	58.26	40.90
+ $RbClO_4$	149.73	137.80	120.45	70.13	57.41	40.98
+ $CsClO_4$	148.77	138.42	119.71	70.20	56.34	41.22

[a] Measured in CD_3CN. [b] C_1−C_4 are designated as 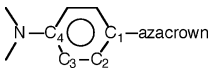

isomers. Likewise, the resonance attributed to the methylene groups next to the macrocyclic N atom and the majority of aromatic resonances shift downfield due to the inductive effect produced by coordination to a cationic guest. However, in contrast to the *ortho* isomers and that of the previously reported *meta*-Wurster's crowns,[38] the noncoordinating distal dimethylamino groups in the *para*-Wurster's crowns give characteristic ^{13}C resonances upfield of those in the free ligands. Thus, the metal binding event is efficiently communicated across the π-system and out to the methyl functionalities. Lacking the pendant donor functionality present in the *ortho* isomers, crowns **16**−**18** give spectra for their metal complexes that more closely align with the cavity sizes of the crowns. Thus, the ^{13}C resonances of the methylene groups next to the macrocyclic N atoms along with most of the others in the spectra of the complexes are shifted the greatest in the Li^+ complex of **16**, the Li^+ and Na^+ complexes of **17**, and the K^+ complex of **18**.

Electrochemistry. The *ortho*- and *para*-TMPD isomers are known to form stable radical cationic and quinoid-like dicationic oxidation states as evidenced by the presence of two reversible redox couples in the cyclic voltammograms of each.[11] Due to steric crowding, the neighboring dimethylamino groups in *o*-TMPD are less able to stabilize the singly oxidized phenylenediamine core. As such, *o*-TMPD oxidizes at a potential that is over 400 mV more anodic than *p*-TMPD. However, the difference in the first and second oxidation potentials is substantially smaller for *o*-TMPD because the steric strain in the radical cation is relieved upon removal of a second electron by forming the nonplanar dication.[44]

(44) Nelsen, S. F.; Clennan, E. L.; Echegoyan, L.; Grezzo, L. A. *J. Org. Chem.* **1978**, *43*, 2621−2628.

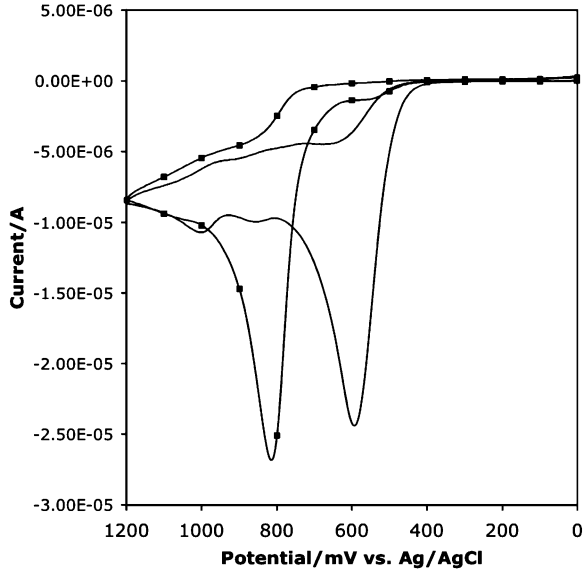

Figure 2. Cyclic voltammograms (0.1 M (TEA)BF_4, CH_3CN, 100 mV/s) of **7** (—) and **7**·$LiBF_4$ (—■—).

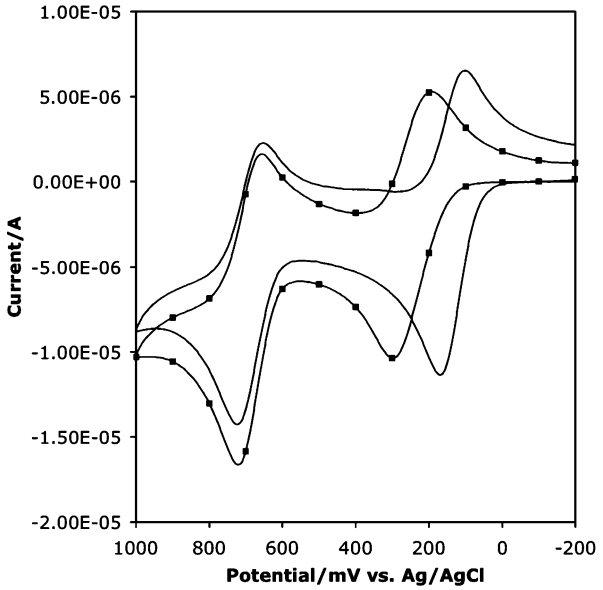

Figure 3. Cyclic voltammograms (0.1 M (TEA)BF_4, CH_3CN, 100 mV/s) of **18** (—) and **18**·KPF_6 (—■—).

The electrochemical properties of ligands **7**−**9** and **16**−**18** were explored by cyclic voltammetry. The *ortho*-Wurster's crowns **7**−**9** oxidize at a comparable potential (606 mV for **7**, 593 mV for **8**, and 582 mV for **9** vs Ag/AgCl) to *o*-TMPD (590 mV)[44] but not reversibly at scan rates of 100 mV/s (see Figure 2). As was previously reported for **9**,[18] at faster scan rates (3 V/s) ligands **7** and **8** show the anticipated two reversible oxidations characteristic of *o*-TMPD with similar half-wave potentials for the two redox processes. As such, while the formal replacement of two methyl groups of *o*-TMPD with a crown subunit has a minimal affect on the oxidation potential of the redox center, it apparently alters the stability of the *o*-phenylenediamine radical. In contrast, *para*-Wurster's crowns **16**−**18** have electrochemical properties nearly identical with that of Wurster's reagent (*p*-TMPD) displaying two reversible one electron oxidations at scan rates of 100 mV/s (see Figure 3).

The coordination of metal cations by redox-active macrocyclic receptors alters the redox potentials of the ligands by "through space" and/or "through bond" interactions between the redox center and bound cation. For crowns that contain oxidizable redox centers of the "neutral-to-cationic" type (e.g., ferrocene, tetrathiafulvalene, and phenylenediamine) the result is an anodic shift in the oxidation potential of the ligand. Thus, the coordination chemistry of the *ortho*- and *para*-Wurster's crowns with alkali metal cations was studied by cyclic voltammetry. A 2 equiv amount of either $LiBF_4$, $NaClO_4$, KPF_6, $RbClO_4$, or $CsClO_4$ was added to each Wurster's crown, and voltammograms were recorded at scan rates of 100 mV/s (0.1 M (TEA)BF_4 in CH_3CN). As shown in Figure 2, the addition of $LiBF_4$ to **7** results in an irreversible oxidation that is 240 mV more anodic than that of the free crown. Unlike the free crown, increasing the scan rate to 3 V/s does not result in two coupled redox processes. The gross features of the voltammogram of **7**·$LiBF_4$ are representative of those for all of the alkali metal complexes of the *ortho*-Wurster's crowns.

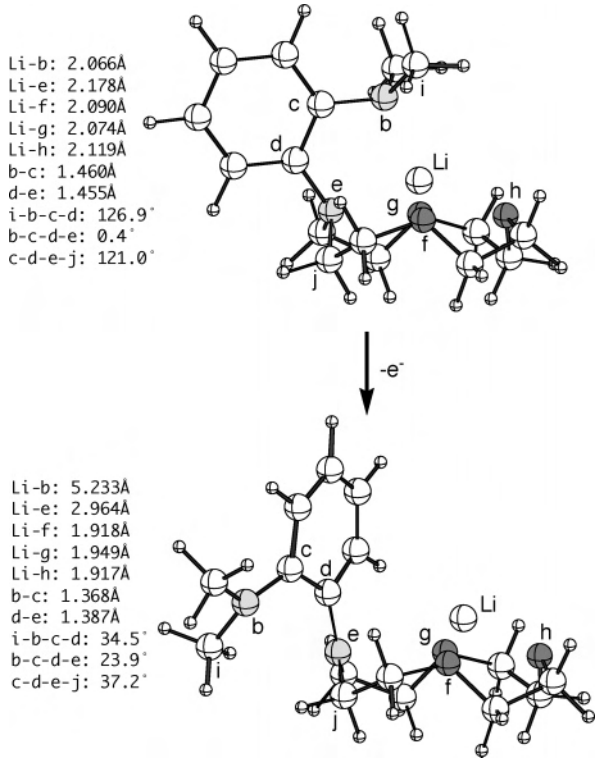

Figure 4. (U)B3LYP/6-31+G*-optimized geometries for **7**·Li^+ in the neutral and radical cation states.

To gain insight into the structural changes that result from the oxidation of *ortho*-Wurster's crown metal complexes, ab initio studies were performed on **7**·Li^+ in the neutral and oxidized states (see Figure 4). The lowest energy conformation of the neutral ligand possesses local C_4 crown symmetry and has the pendant arm situated directly over the binding pocket with the dimethylamino group ligating the metal ion. Upon oxidation, the crown fragment retains the C_4 orientation that favors its interaction with the metal ion while the Coulombic repulsion between the ligand radical cation and the cationic guest favors the pendant arm rotating away from

the binding pocket to maximize the distance between the positive charges. In this context, the Li−b and Li−e interatomic distances increase upon oxidation by 3.167 and 0.786 Å, respectively, while distances Li−f, Li−g, and Li−h decrease by an average of 0.166 Å. Also driving the rotation of the pendant arm is the redox moiety's pursuit of planarity, the orientation in which the dimethylamino group maximizes its ability to stabilize the positive charge of the radical cation through π-donation to the phenyl ring.

In contrast to the *ortho* isomers, the cyclic voltammograms of *para*-Wurster's crown complexes give two reversible oxidation waves with only the first redox couple significantly shifted with respect to the free ligand. For example, the voltammograms of **18** and **18**·KPF_6 are shown in Figure 3. The shifted first redox couple indicates that the radical cation state of **18** is still a viable ligating entity. Because the radical cation of **18** is delocalized, the macrocyclic N atom maintains some Lewis base character and can still participate in stabilizing the metal complex. The unchanged second redox couple is consistent with the loss of the metal ion. The second oxidation places a full positive charge on each N atom of the ligand thereby destabilizing the complex. A recent theoretical study on the alkali metal complexes of **18** in the neutral, oxidized, and doubly oxidized states confirms this interpretation of the voltammetric data.[12e]

In Figure 5, shifts in the first oxidation potentials of the isomeric pairs of *ortho*- and *para*-Wurster's crowns for the entire series studied are plotted vs the ionic radii of the cations. In general, the *ortho*-Wurster's crown platform produces much larger anodic shifts in the oxidation potentials of the ligands upon coordination of alkali metal cations. Indeed, the electrochemical responses are among the highest recorded for alkali metal cations.[7b,8c] This is undoubtedly a direct result of the strong participation of the *o*-phenylenediamine subunit in complex stability via both ligating amino groups. In addition, the magnitudes of the anodic shifts for both sets of crowns reveal selective coordination on the basis of host cavity size. We[38] and Pearson and Hwang[14c] have previously demonstrated relationships between complex stability and electrochemical response for *meta*-Wurster's crowns and piperidine-derived *para*-phenylenediamine crowns, respectively. For the smallest pair of isomeric crowns **7** and **16** (Figure 5a), the Li^+ cation causes the largest shift in oxidation potential with the response of the *ortho*-Wurster's crown more than twice that of the *para* isomer. Complexes of **7** with Na^+ are noted by a more modest shift, whereas there is no electrochemical shift to Na^+ by **16**. No shift in oxidation potential is observed for any of the remaining three alkali metal cations. The larger crowns **8** and **17** show more pronounced shifts for both Li^+ and Na^+ (Figure 5b) with enhanced selectivity for Na^+ vs the smaller analogs **7** and **16**. Interestingly, the *ortho* isomer **8** gives a particularly strong response to Li^+ while the *para* isomer displays plateau selectivity for Li^+ and Na^+. No anodic shifts were observed for the larger alkali metal cations. This is somewhat surprising for K^+ as the ^{13}C NMR data support the formation of K^+ complexes with both crowns and, further, the chelating ability of the *ortho*-phenylenediamine moiety in **8** should be well-suited for stabilizing complexes with metal ions that are larger than the macrocyclic cavity size.

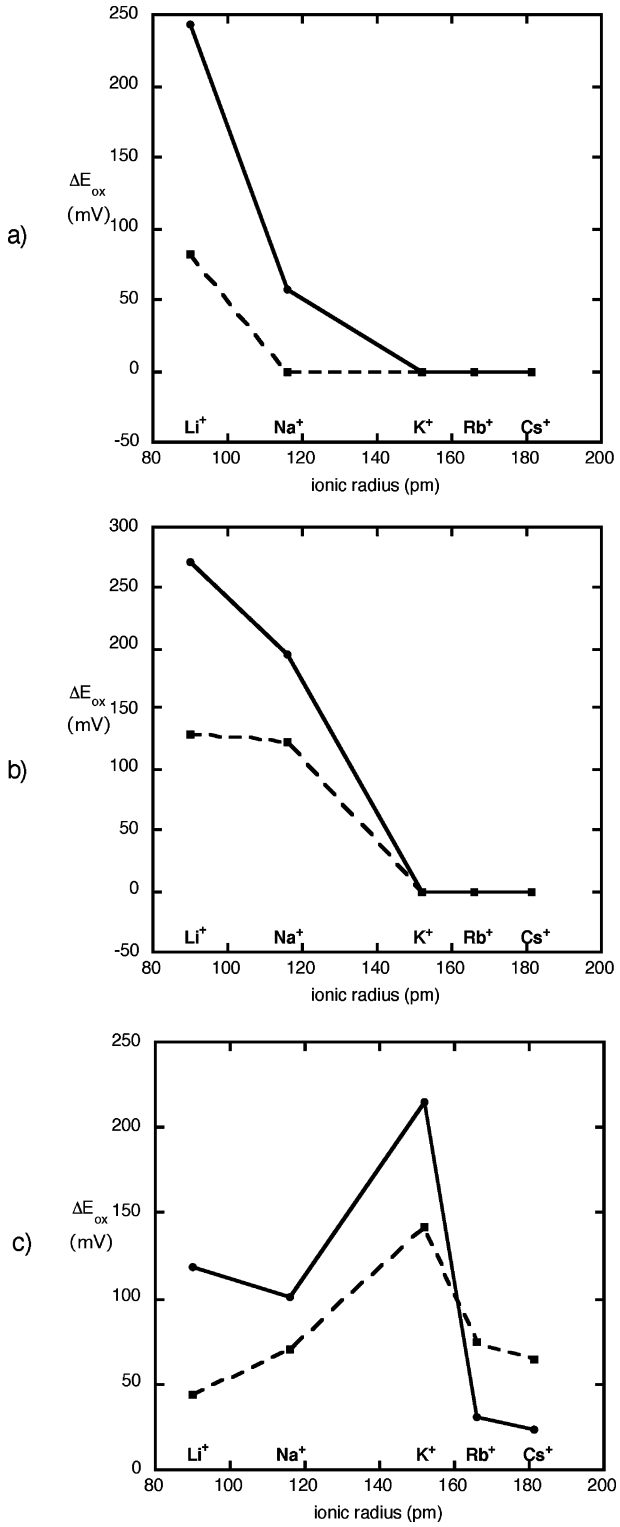

Figure 5. Change in oxidation potential, ΔE_{ox} (0.1 M (TEA)BF_4, CH_3CN, 100 mV/s), vs ionic radius for alkali metal complexes of (a) **7** (−●−) and **16** (---■---), (b) **8** (−●−) and **17** (---■---), and (c) **9** (−●−) and **18** (---■---).

In Figure 5c, the isomeric pair of 18-crown-6 analogs, **9** and **18**, shows clear preference for the K^+ cation. As was observed for **8**, no shift in the oxidation potential of **9** is observed for cations that exceed the optimal match with its

cavity size (i.e., Rb^+ and Cs^+). However, the *para* isomer, **18**, does respond to the larger cations. This is consistent with the ^{13}C NMR data in which larger spectral changes were observed in the complexes of **18** with Rb^+ and Cs^+ vs those for **9**. Like **8**, the larger crown **9** displays an unexpected and comparatively large response to the small lithium cation. Finally, it is worth noting that neither *o*- nor *p*-TMPD shows any change in its voltammograms/oxidation potentials in the presence of the five alkali metal salts used in this study. Thus, all anodic shifts reported here are attributed to the formation of macrocyclic complexes.

Mass Spectrometry. Electrospray mass spectrometry has become a valuable tool for determining relative stabilities of certain types of metal complexes.[45] In particular, alkali metal complexes of crown ethers have been well-studied using this technique. In Figure 6, the relative stabilities of the alkali metal complexes with the *para*-Wurster's crowns **16**−**18** are shown. Samples were prepared by providing a cocktail of alkali metal salts ($LiBF_4$, $NaClO_4$, KPF_6, $RbClO_4$, and $CsClO_4$) in acetonitrile to each ligand such that each cation was present in a stoichiometric excess (>1 equiv vs the ligand). The mixtures were evaporated with the resultant solids dissolved in dichloromethane and filtered. The contents of the filtrates were then analyzed by electrospray mass spectrometry. The mass spectra of crowns **16**−**18** clearly show the influence of cavity size on complex stability as their most prevalent complexes in the competitive binding environment are with Li^+, Na^+, and K^+, respectively. In fact, in Figure 6c, the alkali metal ion binding profile of **18** is nearly identical in relative magnitude with that produced from the voltammetric experiments (see Figure 5c). A similar selectivity was shown for the isomeric meta-Wurster's crowns using the same technique. Unfortunately, attempts to study the alkali metal complexes of the *ortho*-Wurster's crowns proved unsuccessful resulting in data that were not reproducible. While the reason for this is unclear, the lariat ether topology may give rise to large differences in relative complexation rates for the alkali metal cations that contribute significantly in a competitive binding environment.

X-ray Crystallography. To gauge the degree of participation of the phenylenediamine unit in complex stability and probe its impact on the binding ability of the crown unit, we investigated Wurster's crown complexes via X-ray crystallography. To date, there are three reported X-ray structures of Wurster's crown metal complexes[18,40,46] with only one being that of a Wurster's crown ether[18] (complex **9**·KPF_6). In this section, four X-ray structures of Wurster's crown ether complexes are described (Figures 7−10) with Table 4 providing selected bond lengths and angles. Two of the complexes, **8**·$NaPF_6$ and **17**·$NaBF_4$, contain isomeric complex cations and allow for direct comparison of the *ortho*- and *para*-Wurster's crown coordination environments. The other two structures, **8**·KPF_6 and **9**·$LiBF_4$, highlight the ability of the *ortho*-Wurster's crowns to stabilize complexes in which there is a mismatch between cavity and ion size.

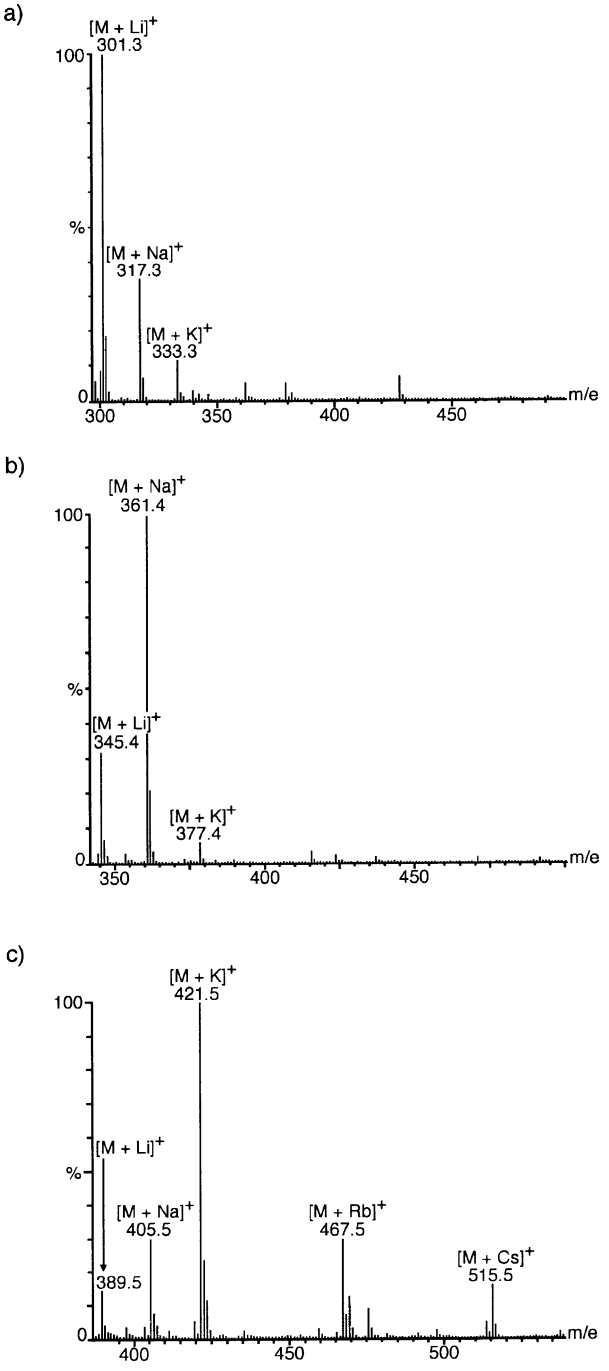

Figure 6. Electrospray mass spectra recorded in the presence of equimolar amounts of Li^+, Na^+, K^+, Rb^+, and Cs^+ ions for (a) **16**, (b) **17**, and (c) **18**.

Structure of 8·$NaPF_6$. Ligand **8** provides a macrocyclic core similar in size and identical in denticity compared to that of 15-crown-5 and, therefore, should be optimal for accommodating the sodium cation. As shown in Figure 7, the structure of **8**·$NaPF_6$ contains the Na^+ cation encapsulated by the crown and ligated by all six available heteroatoms. The average Na−O bond length is 2.382 Å, just slightly below the 2.42 Å average computed for four previously

(45) Sherman, C. L.; Brodbelt, J. S. *Anal. Chem.* **2003**, *75*, 1828−1836 and references therein.
(46) Sibert, J. W.; Forshee, P. B.; Lynch, V. *Inorg. Chem.* **2006**, *45*, 6108−6110.

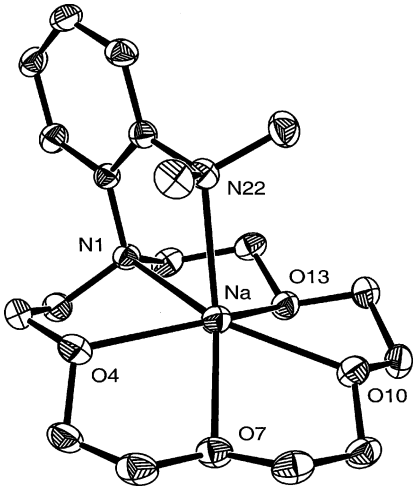

Figure 7. X-ray structure of **8**·$NaPF_6$ (H atoms and PF_6^- anion omitted for clarity). Thermal ellipsoids are plotted at the 50% level.

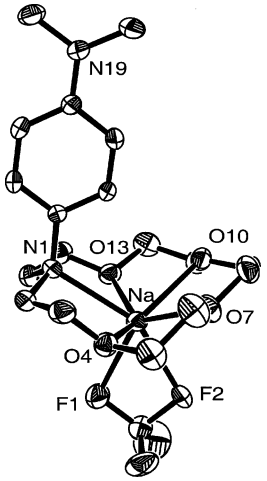

Figure 8. X-ray structure of **17**·$NaBF_4$ (H atoms omitted for clarity). Thermal ellipsoids are plotted at the 50% level.

Table 4. Selected Bond Lengths (Å) and Bond Angles (deg) for **8**·$NaPF_6$, **8**·KPF_6, **9**·$LiBF_4$, and **17**·$NaBF_4$

		8·$NaPF_6$	
Na−N1	2.4478(18)	Na−O7	2.3531(16)
Na−N22	2.4524(19)	Na−O10	2.3686(16)
Na−O4	2.4311(16)	Na−O13	2.3727(16)
C16−N1	1.459(2)	C17−N22	1.453(3)
C16−N1−C2	111.82(15)	C17−N22−C24	110.90(16)
C16−N1−C15	111.57(16)	C17−N22−C23	110.69(16)
C2−N1−C15	111.95(17)	C23−N22−C24	109.38(17)
		8·KPF_6	
K−N1	2.978(3)	K−O7	2.831(3)
K−N17	2.842(3)	K−O10	2.791(3)
K−O4	2.701(3)	K−O13	2.786(3)
K−F1	2.796(4)	K−F2	3.001(5)
C16−N1	1.452(4)	C17−N17	1.440(4)
C16−N1−C2	114.8(3)	C17−N17−C171	112.5(3)
C16−N1−C15	108.9(3)	C17−N17−C172	113.4(3)
C2−N1−C15	110.6(3)	C171−N17−C172	109.4(3)
		9·$LiBF_4$	
Li1−N1	2.185(5)	Li1−O16	2.062(7)
Li1−N25	2.168(5)	Li1−O16a	2.345(8)
Li1−O4	2.055(4)	Li1−O1w	1.914(5)
C20−N25	1.449(3)	C19−N1	1.449(3)
C20−N25−C26	111.09(18)	C19−N1−C18	113.4(4)
C20−N25−C27	111.19(18)	C19−N1−C18a	107.3(5)
C26−N25−C27	110.0(2)	C2−N1−C18	116.8(5)
C19−N1−C2	112.6(2)	C2−N1−C18a	106.9(6)
		17·$NaBF_4$	
Na−N1	2.580(3)	Na−O13	2.389(3)
Na−O4	2.394(3)	Na−F1	2.381(3)
Na−O7	2.417(3)	Na−F2	2.365(14)
Na−O10	2.440(3)	C19−N19	1.383(4)
C16−N1	1.452(4)		

reported Na^+ complexes of 15-crown-5.[47] The sodium cation is drawn above the five macrocyclic donor atoms (0.525 Å) by the apical coordination to the dimethylamino group. The hexafluorophosphate counterion is noncoordinating. The two N atoms of the *o*-phenylenediamine subunit participate nearly equally in the complex with bond lengths of 2.4478(18) and 2.4524(19) Å to N1 and N22, respectively. Additionally, the average C−N−C bond angle in both the dimethylamino group (110.0°) and the macrocyclic amino group (111.8°) is consistent with nearly complete pyramidalization of each nitrogen atom. The strong participation of the chelating phenylenediamine subunit in the solid-state complex mirrors the behavior observed in solution in both the ^{13}C NMR and electrochemical experiments.

Structure of 17·$NaBF_4$. Figure 8 shows the sodium complex of ligand **17**. Similar to the case for **8**·$NaPF_6$, all five macrocyclic donor atoms of **17**·$NaBF_4$ are strongly coordinated to the metal center with an average Na−O distance of 2.408 Å and a Na−N distance of 2.580 Å. The Na^+ atom is disposed 0.871 Å below the macrocyclic donor atom plane with respect to the redox center and is capped by the strongly coordinated BF_4^- counterion. This contrasts with the *ortho* structure, **8**·$NaPF_6$, where the strong interaction with both N atoms of the dimethylamino group served to pull the Na^+ cation to the same side of the crown as the TMPD unit. In addition and unlike that observed for **8**·$NaPF_6$, the noncoordinated dimethylamino appendage maintains sp^2 hybridization ($C-N-C_{av} = 119.9°$). As predicted for *para*-Wurster's crowns by a recently reported theoretical analysis,[12e] the phenyl ring in **17**·$NaBF_4$ is perpendicular to the crown, thereby freeing up the lone pair on the macrocyclic N atom to coordinate to the metal center.

Structure of 8·KPF_6. Despite the NMR and electrochemistry data indicating little to no interaction between **8** and K^+, single crystals of **8**·KPF_6 were obtained serendipitously through slow evaporation of a pentane−chloroform solution. As shown in Figure 9 and in contrast to the previously reported K^+ complex with **9**,[17] the potassium cation is too large to be completely immersed within the cavity of the 15-membered ring, resting 1.458 Å above the plane of the five macrocyclic donor atoms. The potassium cation is sandwiched between the dimethylamino arm and the crown while being coordinated to all of the ligand donor atoms (average K−O distance = 2.777 Å; average K−N distance

(47) (a) Fisher, A. *Z. Kristallogr.* **1996**, *211*, 827−828. (b) Buchanan, G. W.; Gerzain, M.; Bensimon, C. *Acta Crystallogr.* **1994**, *C50*, 1016−1019. (c) Shoham, G.; Cohen, N. *Acta Crystallogr.* **1989**, *C45*, 1154−11158. (d) Weller, F.; Borgholte, H.; Stenger, H.; Vogler, S.; Dehnicke, K. *Z. Naturforsch., B: Chem. Sci.* **1989**, *44*, 1524−1530.

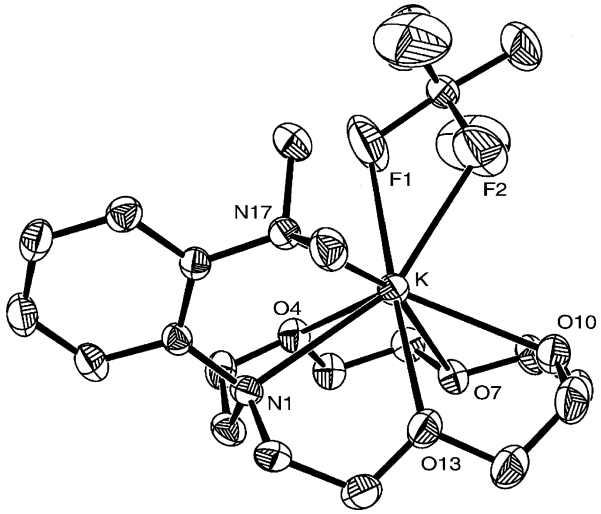

Figure 9. X-ray structure of **8**·KPF_6 (H atoms omitted for clarity). Thermal ellipsoids are plotted at the 50% level.

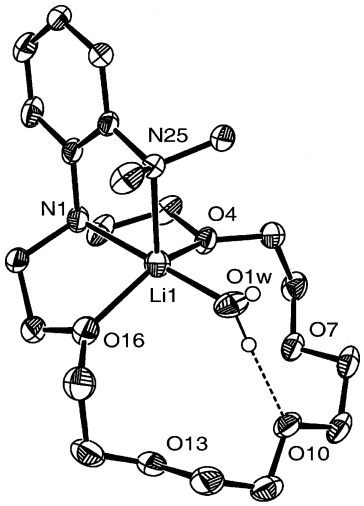

Figure 10. X-ray structure of **9**·$LiBF_4$ (H atoms and BF_4^- anion omitted for clarity). Thermal ellipsoids are plotted at the 50% level.

= 2.885 Å). This results in the redox center being skewed approximately 22° from the near perpendicular orientation with respect to the plane of the crown that is seen in either **8**·$NaPF_6$ or **9**·KPF_6. This arrangement further allows for coordination of the BF_4^- anion on the same side of the crown as the phenylenediamine pendant. Because of the cavity size−atomic radius mismatch, previously reported K^+ complexes with 15-crown-5 are either 2:1 ligand to metal sandwich-type complexes[48] or contain further coordination to the exposed face of the metal cation in 1:1 complexes.[49] The present example fits into the latter category with the observed 1:1 complex due to the additional ligating ability of the *o*-phenylenediamine subunit.

Structure of 9·$LiBF_4$. Single crystals of **9**·$LiBF_4$ were prepared to better understand the solution-phase data (cyclic voltammetry and ^{13}C NMR spectroscopy) suggesting a generally pronounced affinity of the *ortho*-Wurster's crown ethers for Li^+. As shown in Figure 10, the Li^+ ion interacts strongly with both N atoms (2.184 and 2.167 Å for N1 and N25, respectively) and the two O atoms closest to the phenylenediamine moiety, O4 and O16 (average Li−O distance 2.129 Å). The three other O atoms in the crown are noninteracting with Li−O distances in excess of 3.7 Å. Thus, given a choice, the Li^+ cation prefers phenylenediamine chelation vs macrocycle coordination. Presumably, this preference holds for all of the *ortho*-Wurster's crown ethers and explains the large NMR and voltammetric shifts in the Li^+ complexes of **7**−**9**. The coordination sphere of Li^+ is completed by a molecule of H_2O ($Li-O_W$ 1.915 Å) that is further anchored through hydrogen bonding to O10 in the crown framework. It is worth noting that two reported crystal structures of Li^+ complexes with 18-crown-6 show coordination to a subset of macrocyclic O atoms which, similar to **9**·$LiBF_4$, also contain coordinated water molecules hydrogen-bonded to the crown.[50]

Conclusion

In summary, the 12-crown-4, 15-crown-5, and 18-crown-6 analogs of both *ortho*- and *para*-Wurster's crown ethers were prepared and their properties compared. In the case of the *para*-Wurster's crowns, the formal addition of crown ether moieties to *p*-TMPD does not significantly alter the electrochemical properties of the phenylenediamine moiety. In contrast, the *ortho*-Wurster's crowns are less robust electrochemically than *o*-TMPD, though their increased resistance to oxidation in comparison to their *para* counterparts make them ideal candidates for the encapsulation of guests with oxidizing ability.[46] Both sets of ligands showed significant anodic shifts upon exposure to alkali metal cations with selectivity profiles that mirror those of the crown ethers from which they are derived. However, the *ortho* isomers were particularly responsive due to the chelating ability of the *ortho*-phenylenediamine subunit. The strong link between the phenylenediamine component and bound guest ions was demonstrated in solution and the solid state for both the *ortho*- and *para*-Wurster's crowns. Finally, the results of this study demonstrate that replacement of a macrocyclic donor atom with either an *ortho*- or *para*-phenylenediamine moiety does not alter the inherent coordination chemistry of the crown. In other words, ligands **9** and **18**, Wurster's analogs of 18-crown-6, for example, have comparable coordination chemistry to 18-crown-6. This will allow future investigations to take full advantage of the rich history of crown chemistry to prepare a variety of Wurster's crown analogs for sensing and/or redox-switchable applications.

Acknowledgment is made to the Robert A. Welch Foundation (Grant No. AT-1527), the donors of the Petroleum

(48) See, for examples the following: (a) Neumüller, B.; Gahlmann, F.; Schäfer, M.; Magull, S. *J. Organomet. Chem.* **1992**, *440*, 263−275. (b) Lin, S. Y.; Liu, S. W.; Lin, C. M.; Chen, C. H. *Anal. Chem.* **2002**, *74*, 330−335 and references therein.

(49) See, for examples the following: (a) Chadwick, S.; Ruhlandt-Senge, K. *Chem.—Eur. J.* **1998**, *4*, 1768−1780. (b) Dong, T.-Y.; Chang, C.-K.; Cheng, C.-H.; Lin, K.-J. *Organometallics* **1999**, *18*, 1911−1922. (c) Liddle, S. T.; Clegg, W. *Polyhedron* **2002**, *21*, 2451−2455.

(50) (a) Groth, P. *Acta Chem. Scand.* **1982**, *A36*, 109−115. (b) Chang, T.-L.; Zhao, M.; Hu, N.-H.; Jin, Z.-S. *Rev. Chim. Miner.* **1987**, 382−390.

Research Fund, administered by the American Chemical Society (Grant No. 33590-B5), the North Carolina Supercomputer Center, and the ECU Center for Applied Computational Studies (CACS) for their continued support of this research. In addition, we are grateful to Catherine Branch and Doug Ogrin at the Texas Center for Crystallography at Rice University for their help with structures **8**·KPF_6 and **17**·$NaBF_4$ and Northwestern University's Analytical Services Laboratory for the acquisition of mass spectrometry data.

Supporting Information Available: X-ray crystallographic data for **8**·$NaPF_6$, **8**·KPF_6, **9**·$LiBF_4$, and **17**·$NaBF_4$ in CIF format. This material is available free of charge via the Internet at http://pubs.acs.org.

IC701560N